

COMPUTATIONAL HEMODYNAMICS & COMPLEX NETWORKS INTEGRATED PLATFORM TO STUDY INTRAVASCULAR FLOW IN THE CAROTID BIFURCATION

Karol Calò (1), Diego Gallo (1), Valentina Mazzi (1), Stefania Scarsoglio (1), Mohammad O. Khan (2), David A. Steinman (3), Luca Ridolfi (1), Umberto Morbiducci (1)

(1) Polito^{BIOMed} Lab, Department of Mechanical and Aerospace Engineering, Politecnico di Torino, Turin, Italy

(2) Cardiovascular Biomechanics Computation Lab, Department of Pediatrics, Cardiology, Stanford University, Stanford, California, US

(3) Biomedical Simulation Lab, Department of Mechanical & Industrial Engineering, University of Toronto, Toronto, Ontario, Canada

INTRODUCTION

The well-established role of hemodynamics in cardiovascular disease [1] makes the study of cardiovascular flows of wide interest. Here we apply for the first time a method based on complex networks (CNs) theory [2] to investigate and characterize quantitatively the complexity of cardiovascular flows. The rationale lies in the ability of CNs to explore the complexity of physical systems, such as 4D cardiovascular flows, in a synthetic and effective manner. CN-based approaches have already proven useful for data-driven learning of dynamical processes that are hidden to other analysis techniques. In detail, a dataset of 10 patient-specific computational hemodynamics models of human carotid bifurcation (CB) is considered here. Quantitative metrics derived from CNs theory are applied to two fluid mechanics quantities describing the intricate intravascular hemodynamics. These are (1) the so-called axial velocity, i.e. the blood velocity component aligned with the main flow direction, as identified by the vessels centerline, and (2) the kinetic helicity density, a measure of pitch and torsion of the streaming blood. The obtained results suggest the potency of CNs in unveiling fundamental organization principles in cardiovascular flows.

METHODS

Ten patient-specific computational hemodynamics models of CB from the Vascular Aging-The Link That Bridges Age to Atherosclerosis (VALIDATE) study are considered. An overview of the methods is provided in **Figure 1**. Briefly, vascular geometries and flow rates at inflow and outflow boundaries were acquired from contrast-enhanced angiography and phase-contrast MRI. The common carotid artery (CCA) geometry was reconstructed from the thoracic segment, where possible, to well above the bifurcation. On the reconstructed models, uniformly discretized tetrahedral computational

grids were generated, and unsteady-state computational fluid dynamics (CFD) simulations based upon the finite elements method were carried out [3-4]. Additional details are provided elsewhere [3-4].

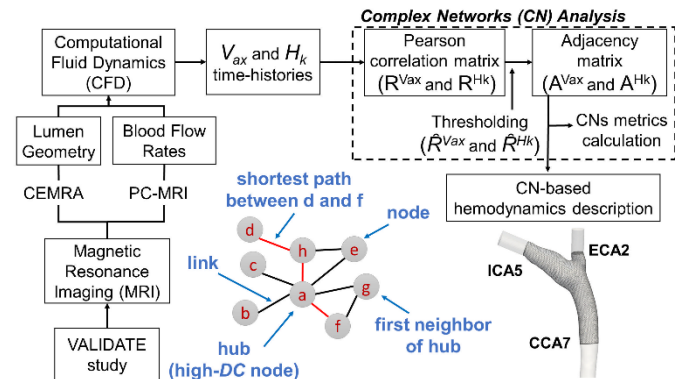


Figure 1: Schematic diagram of the proposed integrated CFD/CNs approach and explanatory example of a CN.

The full-length models were then truncated normal to the branch axis at sections located 7, 2 and 5 radii along respectively the CCA, the external (ECA) and internal (ICA) carotid artery (CCA7, ECA2 and ICA5 sections, respectively, in **Figure 1**), to ensure a consistent spatial extent across all cases [4]. To describe the complexity of intravascular hemodynamics, two fluid mechanics quantities are considered, axial velocity (V_{ax}) and kinetic helicity density (H_k). In detail, V_{ax} is representative of the main flow direction and was calculated by projecting the velocity vector field along the local vessel centerline [5]. The pseudoscalar H_k , defined as the internal product between velocity and vorticity vectors, is considered here due to the recognized

atheroprotective significance of helicity in the CB [4] and, in general, in the evolution and stability of both turbulent and laminar flows. Here CNs are applied to the time-histories of these quantities at each grid node along the cardiac cycle to unveil fundamental organization principles in the CB hemodynamics. In graph theory, a CN is a network with significant patterns of connection between its elements and nontrivial topological features (an explanatory example is presented in **Figure 1**). The CN is defined by a set of nodes $V = 1, \dots, N$ and a set of links E between nodes $\{i, j\}$. In this study the nodes of each CN are represented by the grid points of the finite element mesh used to perform the CFD simulations. For each CB model, the network is built by applying a correlation criterion [6-7]: for each pair of nodes $\{i, j\}$ of the discretized fluid domain, the linear Pearson correlation coefficient R_{ij} is calculated between time-histories of V_{ax} and H_k . Then, the corresponding network is built up based upon the constraint that a topological link between nodes i and j does exist if and only if R_{ij} is greater than a threshold value \hat{R} . The threshold values are set equal to the median of the overall R_{ij} distributions ($\hat{R}^{V_{ax}}=0.55$, $\hat{R}^{H_k}=0$). The obtained network is represented by its adjacency matrix:

$$A_{ij} = \begin{cases} 0, & \text{if } \{i, j\} \notin E \text{ or } i = j, \\ 1, & \text{if } \{i, j\} \in E. \end{cases} \quad (1)$$

A_{ij} contains all the information about node connectivity: $A_{ij}=1$ if a link does exist between node i and node j ($R_{ij} > \hat{R}$); $A_{ij}=0$ elsewhere. On the built up networks, we calculated the following several CNs metrics: (1) the *degree centrality* (DC_i) of node i , defined as the fraction of nodes of the network directly connected to node i (the so-called first neighborhood of node i); (2) the *diameter* D of the network, defined in terms of number of links as the maximum value of the shortest path length between nodes i and j (**Figure 1**, in red); (3) the *Average Euclidean Distance* (AED_i) [6] of node i from all its first neighbors $n(i)$. AED provides a quantitative evaluation of the length of persistence of the correlation of hemodynamic structures inside the vascular domain, and their main direction of propagation. Intravascular structures characterized by high AED keep their correlation high within a large spatial distance, on the other hand for low AED structures the correlation vanishes within a shorter distance.

RESULTS

The volumetric maps of the V_{ax} degree centrality DC are presented in **Figure 2** for all the investigated CB models. In general, for V_{ax} high DC values characterize the nodes in the CCA, while nodes located at the carotid bulb present lower DC values. In most cases, high correlation among V_{ax} time-histories is restored distally to the flow divider, in ECA and ICA. On average, the value of the network diameter D is equal to 4 (range 3-5) for the ten investigated cases. Notably, the models presenting the highest and the lowest value for D are the same presenting respectively the highest and lowest value of carotid flare, a measure of the geometric expansion of the carotid bulb and known trigger of flow disturbances. The volumetric map for AED metric for a representative model is also displayed in **Figure 2**. In detail, AED map reveals that V_{ax} time-histories of nodes located close to CCA7 and ICA5 sections are characterized by a neighborhood that expands on a distance equivalent to 3 CCA7 diameters (d_{CCA7}) or more, while shorter AED characterize nodes located in the carotid bulb. The CN-based analysis on H_k highlighted in all the models that two balanced, distinguishable positively/negatively correlated regions emerge from the distribution of DC values, which represent the detailed picture of those counter-rotating helical flow structures visualized and described in terms of integral quantities in previous studies [4]. All H_k networks are characterized by $D = 2$, i.e. the most

distant nodes are separated only by a two-links path. Lastly, from the AED results, it emerged that H_k time-histories with the largest AED (equal to $3.5 d_{CCA7}$) are located close to the CCA7 and ICA5 sections. Interestingly, in general helical flow structures exhibit shorter AED values, i.e., shorter length of persistence of the correlation, in the bulb region, similarly to what was observed for V_{ax} .

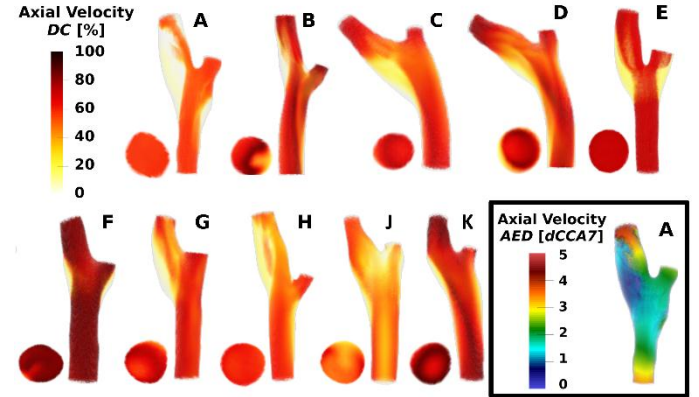


Figure 2: Volumetric maps of DC for all the ten V_{ax} networks, and volumetric distribution of AED for one representative model.

DISCUSSION

The CNs analysis on V_{ax} allows one to isolate two distinct regions, i.e., an “undisturbed” hemodynamic region vs. a “disturbed” hemodynamic region. The former presented high DC and AED values, physically implying that in that region forward flow dominates and V_{ax} time-histories are highly correlated, and this correlation is kept for large distances. The “undisturbed” hemodynamic region represents the largest fraction of the nodes, as DC values are $>80\%$. On the other hand, the “disturbed” hemodynamic region corresponds to the carotid bulb, where the propensity to plaque formation is stronger. There, only a smaller fraction of nodes is highly correlated (lower DC values), expanding for an AED of about one CCA7 diameter. The observed correspondence between metric D and the carotid flare suggests that the expansion at the bifurcation, markedly contributing to break up the topological links of the network, is the putative mechanism of correlation dispersion of V_{ax} . As far as H_k is concerned, CNs analysis emphasizes the presence of two distinguishable, balanced counter-rotating helical structures [4] as an emergent feature in CB hemodynamics, showing that in the bulb helical patterns maintain correlation on a much shorter distance than elsewhere. This aspect confirms (in such a way that can be measured in terms of persistence length of the correlation within the fluid domain) the role of the carotid sinus in promoting complex flow structures. In conclusion, the proposed integrated CFD-CN-based approach has the potential to provide a more complete picture of the intravascular flow complexity/disturbances, quantifiable in terms of persistence length of correlated hemodynamic quantities.

REFERENCES

- [1] Morbiducci, U et al., *Thromb Haemost*, 115:484-92, 2016.
- [2] Boccaletti, S et al., *Phys Rep*, 424:175-308, 2006.
- [3] Hoi, Y et al., *Physiol Meas*, 31:291-302, 2010.
- [4] Gallo, D et al., *Ann Biomed Eng*, 43(1):68-81, 2015.
- [5] Morbiducci, U et al., *J Biomech*, 48(6):899-906, 2015.
- [6] Scarsoglio, S et al., *Int J Bifurcation and Chaos*, 26(13), 1650223:1-12, 2016.
- [7] Iacobello, G et al., *Phys Rev E*, 98(1), 013107, 2018.